

M₄X₄ Structures in Transition Metal Chemistry: Cubane-like or Planar? A DFT Study of Some Clusters Containing the M₄X₄ Core (M = Ti, V, Mo; X = N, P, As)

JosePedro Sarasa,[†] Josep M. Poblet,^{*,§} and Marc Bénard[‡]

Departamento de Química Física y Química Orgánica, Universidad de Zaragoza, Spain,
 Departament de Química Física i Inorgànica, Universitat Rovira i Virgili,
 43005 Tarragona, Spain, and Laboratoire de Chimie Quantique, UMR 7551, CNRS and
 Université Louis Pasteur, 4, Rue Blaise Pascal, 67000 Strasbourg, France

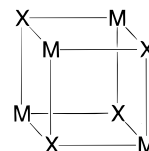
Received December 13, 1999

DFT calculations have been carried out on the organometallic clusters $[(\eta\text{-C}_5\text{H}_5)\text{TiN}]_4$ and $[\text{Cl}_3\text{MoN}]_4$ with the aim of comparing the energies and the electronic structures of the cubane and planar forms for these two clusters. Calculations indicate for the titanium cluster that the cubane conformation is much more stable than the structure in which the four metals and the four nitrogens are in the same plane, whereas the square planar structure is preferred for the molybdenum complex. The octahedral coordination of the metal in the cubane-like form implies an important reorganization of the $[\text{Cl}_3\text{MoN}]$ unit. The high cost of this reorganization explains the relative stability of the square planar conformation in that case. Metal–metal interactions have been characterized in the vanadium cubanes $[(\eta\text{-C}_5\text{H}_5)\text{V}(\mu_3\text{-X})_4]$, X = N, P, and As. The distortion of the cage observed in some cubanes is discussed in relation to the metal–metal bonding interactions evidenced in these clusters.

Introduction

Clusters containing the M₄X₄ core where M is a transition metal and X is an element of group 16 or 17 are quite common.^{1,2} However, clusters with X belonging to group 15 are not so frequent. Dahl and co-workers characterized in the early 1970s the compounds $[\text{Co}(\text{CO})_3(\mu_3\text{-Sb})]_4$ ^{3a} and $[(\eta\text{-C}_5\text{H}_5)\text{Co}(\mu_3\text{-P})]_4$,^{3b} which were the first organometallic clusters to contain group 15 elements in a cubane-like structure (see Chart 1). Later, the X-ray characterization of $[\text{Co}(\text{CO})_3(\mu_3\text{-Bi})]_4$ showed

Chart 1



that its structure is also cubane-like.^{3c} More recently, Mena and co-workers synthesized the clusters $[(\eta\text{-C}_5\text{Me}_5)\text{Ti}(\mu_3\text{-N})]_4$ and $[(\eta\text{-C}_5\text{Me}_5)\text{Ti}(\mu_3\text{-CH})]_4$, two cubane-like compounds in which the metal atoms are formally d⁰.⁴ At the same time, Bottomley et al. reported the structure of $[(\eta\text{-C}_5\text{Me}_5)\text{V}(\mu_3\text{-N})]_4$, a cluster with similar topology containing four metal electrons.⁵ The diamagnetism of this vanadium cluster was explained from EHT calculations. Several clusters of manganese(II) $[\text{R-Mn}(\mu_3\text{-N-R}')_4]$, in which a R' group is attached to the N atom, have been synthesized by Dehnicke and co-workers.^{6–8} Related clusters of Co(II),^{8,10} Ni(II),⁷ and Zn(II)^{9,10} have also been prepared by the same group.

[†] Universidad de Zaragoza.

[§] Universitat Rovira i Virgili.

[‡] CNRS and Université Louis Pasteur.

(1) See for example: Coucouvanis, D. *Acc. Chem. Res.* **1991**, *24*, 1. Holm, R. H. *Adv. Inorg. Chem.* **1992**, *38*, 1. Saito, T. *Adv. Inorg. Chem.* **1996**, *44*, 45. Ogino, H.; Inomata, S.; Tobita, H. *Chem. Rev.* **1998**, *2093*.

(2) Rundle, R. E.; Sturdivant, J. H. *J. Am. Chem. Soc.* **1947**, *69*, 1561. Evans, J. A.; Kemmitt, R. D. W.; Kimura, B. Y.; Russell, D. R. *J. Chem. Soc., Chem. Commun.* **1972**, 509. Churchill, M. R.; Donahue, J.; Rotella, F. J. *Inorg. Chem.* **1976**, *15*, 2752. Schramm, V. *Inorg. Chem.* **1978**, *17*, 714. Churchill, M. R.; Davies, G.; El-Sayed, M. A.; Hutchinson, J. P.; Rupich, M. W. *Inorg. Chem.* **1982**, *21*, 995. Goel, R. G.; Beauchamp, A. L. *Inorg. Chem.* **1983**, *22*, 395. Rath, N. P.; Holt, E. M.; Tanimura, K. *Inorg. Chem.* **1985**, *24*, 3934. Burch, R. R.; Harlow, R. L.; Ittel, S. D. *Organometallics* **1987**, *6*, 982. Fagan, P. J.; Mahoney, W. S.; Calabrese, J. C.; Williams, I. D. *Organometallics* **1990**, *9*, 1843. Attar, S.; Bowmaker, G. A.; Alcock, N. W.; Frye, J. S.; Bearden, W. H.; Nelson, J. H. *Inorg. Chem.* **1991**, *30*, 4743. Koelle, U.; Kang, B.-S.; Englert, U. *J. Organomet. Chem.* **1991**, *420*, 227. Hakansson, M.; Jagner, S.; Clot, E.; Eisenstein, O. *Inorg. Chem.* **1992**, *31*, 5389. Olson, S.; Helgesson, G.; Jagner, S. *Inorg. Chim. Acta* **1994**, *217*, 15. du Mont, W.-W.; Karnop, M.; Mahnke, J.; Martens, R.; Druckenbrodt, C.; Jeske, J.; Jones, P. G. *Chem. Ber.* **1997**, *130*, 1619. Herberich, G. E.; Eckenrath, H. J.; Englert, U. *Organometallics* **1997**, *16*, 4292. Donath, H.; Avtomonov, E. V.; Sarraje, I.; von Dahlen, K.-H.; El-Essawi, M.; Lorberth, J.; Seo, B.-S. *J. Organomet. Chem.* **1998**, *559*, 191.

(3) (a) Foust, A. S.; Dahl, L. F. *J. Am. Chem. Soc.* **1970**, *92*, 7337. (b) Simon, G. L.; Dahl, L. F. *J. Am. Chem. Soc.* **1973**, *95*, 2175. (c) Ciani, G.; Moret, M.; Fumagalli, A.; Martinengo, S. *J. Organomet. Chem.* **1989**, *362*, 291.

(4) (a) Gómez-Sal, P.; Martín, A.; Mena, M.; Yélamos, C. *J. Chem. Soc., Chem. Commun.* **1995**, 2185. (b) Andrés, R.; Gómez-Sal, P.; de Jesús, E.; Martín, A.; Mena, M.; Yélamos, C. *Angew. Chem., Int. Ed. Engl.* **1997**, *36*, 115. (c) Abarca, A.; Gómez-Sal, P.; Martín, A.; Mena, M.; Poblet, J.-M.; Yélamos, C. *Inorg. Chem.* **2000**, *39*, 642.

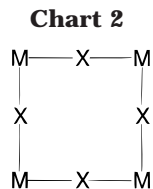
(5) Abernethy, C. D.; Bottomley, F.; Decken, A.; Cameron, T. S. *Organometallics* **1996**, *15*, 1758.

(6) Riese, U.; Neumüller, B.; Faza, N.; Massa, W.; Dehnicke, K. *Z. Anorg. Allg. Chem.* **1997**, *623*, 351. Mai, H.-J.; Neumüller, B.; Dehnicke, K. *Z. Naturforsch.* **1996**, *51b*, 433.

(7) Mai, H.-J.; Kang, H.-C.; Wocadlo, S.; Massa, W.; Dehnicke, K. *Z. Anorg. Allg. Chem.* **1995**, *621*, 1963.

(8) Mai, H.-J.; Meyer zu Köcker, R.; Wocadlo, S.; Massa, W.; Dehnicke, K. *Angew. Chem., Int. Ed. Engl.* **1995**, *34*, 1235.

(9) Krieger, M.; Harms, K.; Magull, J.; Dehnicke, K. *Z. Naturforsch.* **1997**, *52b*, 243. Krieger, M.; Gould, R. O.; Harms, K.; Parsons, S.; Dehnicke, K. *Chem. Ber.* **1996**, *129*, 1621.



[Fe(CO)₃(μ₃-AsCH₃)₄] and [Ru(CO)₃(μ₃-PCF₃)₄] are the only group 8–group 15 cubanes characterized from X-ray diffraction.^{11,12} This variety in the metals and in the ligands external to the cubane core results in a great diversity of the metal valence electron (MVE) counts as defined by Wade and Mingos.¹³ For M₄X₄ clusters where X is a group 15 element, the MVE count varies from 56 electrons in [(η-C₅Me₅)Ti(μ₃-N)]₄, none of which is formally assigned to the metal atoms, up to 80 electrons in [Co(CO)₃(μ₃-Sb)]₄, including 24 metal electrons.

Another set of metal–nitrogen clusters with [R-M(μ₂-N)]₄ formula and square planar structures involve metal–nitrogen bonding either unsymmetrical (M≡N–M bridges with M = Mo^{14–16} and W,^{17–18} Chart 2) or symmetrical (M=N=M as in [(CH₃)₂OPS₂MoN]₄).¹⁹ Different structures have also been found for clusters containing the M₄(μ-X)₆ core, with X = O or Se. Although most of them have an adamantane-like conformation with *T_d* symmetry,²⁰ a *D_{2h}* structure with the metal atoms in a rectangular conformation has been proposed for [(η-C₅Me₅)Nb]₄(μ-O)₆ from the NMR spectra.²¹ Ab initio calculations carried out in our group showed that the *D_{2h}* structure is more stable than the tetrahedral conformation, in agreement with the experimental data.²² In the case of the analogue vanadium cluster, for which an adamantane-like geometry has been observed,²³ the calculations however indicated that the *D_{2h}* form is the most stable one for [(η-C₅H₅)V]₄(μ-O)₆. The theoretical results were reconciled with the observed structure when considering the steric strain induced by the four bulky C₅Me₅ ligands in the *D_{2h}* form. The goal of the present study is to carry out DFT calculations on the model system [(η-C₅H₅)Ti(μ₃-N)]₄ and on the real complex [Cl₃MoN]₄ in order to compare the

cubane with the planar structure for two clusters containing the M₄N₄ core and exemplifying each conformational type, respectively. An analysis of the metal-centered frontier orbitals and of their respective populations in the [(η-C₅H₅)V(μ₃-X)]₄ series (X = N, P, As) will allow an understanding of the distorted geometry and the electronic configuration of the dicapped cubane compound [(η-C₅H₅)V(μ₃-P)]₄(μ-P)₂.²⁴

Computational Details

All calculations have been carried out by means of density functional calculations including gradient corrections. We used the local spin density approximation characterized by the electron gas exchange (Xα with α = 2/3) together with Vosko–Wilk–Nusair²⁵ parametrization for correlation. Becke's non-local corrections to the exchange energy²⁶ and Perdew's nonlocal corrections to the correlation energy²⁷ have been added. Those calculations have been carried out with the ADF program,²⁸ using triple-ζ + polarization Slater basis sets to describe the valence electrons of C, N, P, As, and H. For metal atoms, a frozen core composed of the 1s to 2sp shells for titanium and vanadium, 1s to 3spd shells for molybdenum, and 1s to 4spd for tungsten was described by means of single Slater functions. *ns* and *np* electrons were described by double-ζ Slater functions, *nd* and (*n*+1)*s* by triple-ζ functions, and (*n*+1)*p* by a single orbital.^{29,30} As in the very accurate work of Rosa et al.³¹ on the dissociation of Mn₂(CO)₁₀, it was not found necessary to supplement the metal basis set with f-type polarization functions. Spin-unrestricted calculations were used for the open shell configurations. Calculations for the cubane clusters (Chart 1) have been carried out under the constraints of the *D_{2d}* symmetry group, whereas calculations for the conformation in which the metal and N atoms are coplanar (Chart 2) were carried out with the constraints of the *C_{4v}* symmetry group.

Results and Discussion

[(η-C₅H₅)Ti(μ₃-N)]₄. The geometry computed for the ground state of [(η-C₅H₅)Ti(μ₃-N)]₄ corresponds to an almost perfect cube. The optimized titanium–nitrogen distances for this cubane structure (1.941 and 1.937 Å) are almost identical to the Ti–N distances reported for [(η-C₅Me₅)Ti(μ₃-N)]₄ (1.939 Å).^{4a} The distance from the metal to the centroid of the Cp ring is computed to be 2.138 Å, a value that is also very close to the experimental distance of 2.091 Å. For the nonbonding Ti–Ti and N–N distances the agreement between the optimized (2.80 and 2.68 Å) and experimental (2.79 and 2.69 Å) values is also almost perfect.

(10) Abram, S.; Abram, U.; Meyer zu Köcker, R.; Dehnicke, K. Z. *Anorg. Allg. Chem.* **1996**, 622, 867.

(11) Röttinger, E.; Vahrenkamp, H. *Angew. Chem., Int. Ed. Engl.* **1978**, 17, 273. Röttinger, E.; Vahrenkamp, H. *J. Organomet. Chem.* **1981**, 213, 1.

(12) Ang, H.-G.; Ang, K.-W.; Ang, S.-G.; Rheingold, A. L. *J. Chem. Soc., Dalton Trans.* **1996**, 3131.

(13) Mingos, D. M. P.; Wales, D. J. *Introduction to Cluster Chemistry*; Prentice Hall: Englewood Cliffs, NJ, 1990; and references therein.

(14) Müller, U.; Kujanek, R.; Dehnicke, K. Z. *Anorg. Allg. Chem.* **1982**, 495, 127.

(15) Figge, R.; Friebe, C.; Patt-Siebel, U.; Müller, U.; Dehnicke, K. Z. *Naturforsch.* **1989**, 44b, 1377.

(16) Herrmann, W. A.; Bogdanovic, S.; Behm, J.; Denk, M. J. *Organomet. Chem.* **1992**, 430, C33.

(17) Ergezinger, C.; El-Kholi, A.; Müller, U.; Dehnicke, K. Z. *Anorg. Allg. Chem.* **1989**, 568, 55.

(18) Görg, A.; Patt-Siebel, U.; Müller, U.; Dehnicke, K. Z. *Naturforsch.* **1989**, 44b, 903.

(19) Noble, M. E.; Folting, K.; Huffman, J. C.; Wentworth, R. A. D. *Inorg. Chem.* **1982**, 21, 3772.

(20) Bottomley, F.; Day, R. W. *Organometallics* **1991**, 10, 2560. Harper, J. R.; Rheingold, A. L. *J. Am. Chem. Soc.* **1990**, 112, 4037. Bottomley, F.; Chen, J.; Preston, K. F.; Thompson, R. C. *J. Am. Chem. Soc.* **1994**, 116, 7989.

(21) Bottomley, F.; Boyle, P. D.; Karslioglu, S.; Thompson, R. C. *Organometallics* **1993**, 12, 4090.

(22) Sarasa, J. P.; Poblet, J. M.; Rohmer, M.-M.; Bénard, M. *Organometallics* **1995**, 14, 5665.

(23) Bottomley, F.; Magill, C. P.; Zhao, B. *Organometallics* **1990**, 9, 1700. Bottomley, F.; Magill, C. P.; Zhao, B. **1991**, 10, 1946.

(24) Herberhold, M.; Frohmader, G.; Milius, W. *J. Organomet. Chem.* **1996**, 522, 185.

(25) Vosko, S. H.; Wilk, L.; Nusair, M. *Can. J. Phys.* **1980**, 58, 1200.

(26) Becke, A. D. *J. Chem. Phys.* **1986**, 84, 4524. Becke, A. D. *Phys. Rev.* **1988**, A38, 3098.

(27) Perdew, J. P. *Phys. Rev.* **1986**, B33, 882. Perdew, J. P. **1986**, B34, 7406.

(28) ADF 2.01-2.2; Theoretical Chemistry Vrije Universiteit, Amsterdam. Baerends, E. J.; Ellis, D. E.; Ros, P. *Chem. Phys.* **1973**, 2, 41. te Velde, G.; Baerends, E. J. *J. Comput. Phys.* **1992**, 99, 84. Fonseca-Guerra, C.; Visser, O.; Snijders, J. G.; te Velde, G.; Baerends, E. J. *METECC-95*; Clementi, E., Corongiu, G., Eds.; STEF: Cagliari, Italy, 1995; pp 305–395.

(29) Snijders, J. G.; Baerends, E. J.; Vernooijs, P. *At. Nucl. Data Tables* **1982**, 26, 483.

(30) Vernooijs, P.; Snijders, J. G.; Baerends, E. J. *Slater type basis functions for the whole periodic system*; Internal Report; Free University of Amsterdam, The Netherlands, 1981.

(31) Rosa, A.; Ricciardi, G.; Baerends, E. J.; Stufkens, D. J. *Inorg. Chem.* **1996**, 35, 2886.

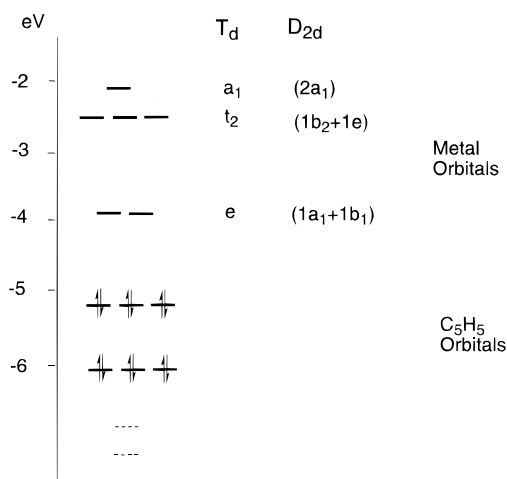


Figure 1. Orbital diagram for $[(\eta\text{-C}_5\text{H}_5)\text{Ti}(\mu_3\text{-N})]_4$.

The formal oxidation state for titanium atoms in the cubane structure of $[(\eta\text{-C}_5\text{Me}_5)\text{Ti}(\mu_3\text{-N})]_4$ is IV. In full agreement with this assignment, the block of d metal orbitals occurs first in the unoccupied set of $[(\eta\text{-C}_5\text{H}_5)\text{Ti}(\mu_3\text{-N})]_4$, whereas the highest occupied molecular orbitals are symmetry-adapted orbitals of the Cp ligands. A scheme of the frontier orbitals including their orbital energies and symmetries is displayed in Figure 1. In this work, the orbitals and electronic configurations were classified using the symmetry properties of the T_d group since the M_4X_4 core has an almost tetrahedral symmetry. However, it is necessary in some cases to use the actual symmetry of the molecule (D_{2d}). In those cases we explicitly indicate that the symmetry labels correspond to the D_{2d} symmetry group. In Figure 1 the two sets of labels were included. Two consequences arise from the lack of metal electrons:

(1) The relatively short Ti–Ti distances (~ 2.8 Å) must be attributed to important metal–ligand interactions and not to direct titanium–titanium couplings.

(2) With no more than 12 electrons in their coordination sphere, the titanium atoms are highly unsaturated and show a strong tendency to accept electrons. This is fully consistent with the presence of low-lying unoccupied orbitals and with the high value computed for the adiabatic electron affinity of $[(\eta\text{-C}_5\text{H}_5)\text{Ti}(\mu_3\text{-N})]_4$ (2.14 eV).

The optimization process for the planar D_{2h} conformation yielded a structure in which all of the Ti–N distances are equal to 1.812 Å. Calculations were also carried out in order to find the alternative structure with the bridging N atoms asymmetrically bonded to the Ti atoms (Ti–N≡Ti). However, the optimization process always yielded structures very close to the D_{2h} conformation with the Ti–N bonds all identical. The energy of this structure is very high ($+123$ kcal mol $^{-1}$) with respect to the cubane conformation. As in the cubane structure, the lowest unoccupied orbitals are d-titanium orbitals, whereas the highest occupied molecular orbitals are combinations of atomic orbitals centered on the N and C atoms. Therefore, we are led to the conclusion that the oxidation state of the titanium atoms in the D_{2h} conformation is also IV, which implies that the nitrogen atoms are assigned a formal charge of -3 . The Mulliken charge computed for the planar conformation is -0.99 . This should be compared to the

Mulliken charges of $-0.53e$ on the triply bonded nitrogen in the $\text{N}\equiv\text{Ti}\text{--Cp}$ monomer and of $-0.87e$ in the cubane conformation of the tetramer. In this latter complex, the nitrogen atoms are formally N^{3-} as in the planar form, but this charge is more delocalized through donation interactions to three metal centers.

The identity of the eight titanium–nitrogen bonds found in the planar form of $[(\eta\text{-C}_5\text{H}_5)\text{Ti}(\mu_3\text{-N})]_4$ makes this conformation geometrically different from the planar structure observed for the isoelectronic complexes $[\text{MnCl}_3]_4$ ($\text{M} = \text{Mo}, \text{W}$) and characterized by a strong alternation of the metal–nitrogen bond lengths.^{32,36} Wheeler et al explained the M–N bond alternation in the $[\text{MnCl}_4]_4^{4-}$ complexes with planar framework by a second-order Jahn–Teller distortion involving the N-localized HOMO and the metal-based LUMO of the tetramer.³⁹ These nonbonding orbitals respectively belonging to the b_{2g} and to the b_{1g} representations of the D_{4h} point group are allowed to undergo a second-order mixing when the symmetry is decreased to C_{4h} . The extent of this distortion is monitored by the HOMO–LUMO gap.³⁹ For the molybdenum complexes investigated by Wheeler et al, the frontier orbitals in the D_{4h} conformation are close in energy and the second-order Jahn–Teller effect is an efficient driving force to the distortion through an enhancement of the metal–nitrogen π bonds. In planar $[(\eta\text{-C}_5\text{H}_5)\text{Ti}(\mu_3\text{-N})]_4$, the interaction between the metal and the Cp rings destabilizes the in-plane combination of the metal d_{xy} orbitals with b_{1g} symmetry. The energy gap with the N-centered HOMO rises to almost 3 eV, and the tendency toward distortion vanishes accordingly. The important energy difference between the planar and the cubane structures is explained by the attractive term gathering the effects of the Coulombic interaction, the mutual polarization, and the orbital interactions among the four monomers. This attractive term is intrinsically higher in the compact cubane-like isomer, and the difference is only partially offset by the steric and Pauli repulsive contributions. We will come back to this point in more detail when the relative stabilities of the tetrameric structures are discussed.

$[(\eta\text{-C}_5\text{H}_5)\text{V}(\mu_3\text{-N})]_4$. The cluster obtained by replacing Ti by V in $[(\eta\text{-C}_5\text{Me}_5)\text{Ti}(\mu_3\text{-N})]_4$ also has a cubane conformation.⁵ As for the titanium cluster, the present DFT calculations reproduce very well the experimental

(32) Walker, I.; Strähle, J.; Ruschke, P.; Dehnicke, K. *Z. Anorg. Allg. Chem.* **1982**, *87*, 26. Musterle, W.; Strähle, J.; Liebelt, W.; Dehnicke, K. *Z. Naturforsch.* **1979**, *B34*, 942.

(33) Rohmer, M.-M.; Bénard, M.; Bo, C.; Poblet, J. M. *J. Am. Chem. Soc.* **1995**, *117*, 508. Rohmer, M.-M.; Bénard, M.; Poblet, J. M. In *Metal Clusters in Chemistry*; Braunstein, P.; Oro, L. A.; Raithby, P. R., Eds.; Wiley-VCH: Weinheim, Germany, 1998; pp 1664–1710. Rohmer, M.-M.; Bénard, M.; Poblet, J. M. *Chem. Rev.* **2000**, *100*, 495.

(34) Bader, R. F. W. *Atoms in Molecules, a Quantum Theory*; Clarendon Press: Oxford, 1990. Bader, R. F. W.; MacDougall, P. J.; Lau, C. D. *J. Am. Chem. Soc.* **1984**, *106*, 1594.

(35) Bo, C.; Sarasa, J.-P.; Poblet, J.-M. *J. Phys. Chem.* **1993**, *97*, 6362.

(36) Strähle, J. *Z. Anorg. Allg. Chem.* **1970**, *375*, 238. Strähle, J. *Z. Anorg. Allg. Chem.* **1971**, *380*, 96.

(37) Strähle, J.; Weiher, U.; Dehnicke, K. *Z. Naturforsch. B* **1978**, *33*, 1347.

(38) For review articles, see: Dehnicke, K.; Strähle, J. *Angew. Chem., Int. Ed. Engl.* **1981**, *20*, 413. Dehnicke, K.; Strähle, J. *Angew. Chem., Int. Ed. Engl.* **1992**, *31*, 955.

(39) Wheeler, R. A.; Whangbo, M.-H.; Hughbanks, T.; Hoffmann, R.; Burdett, J. K.; Albright, T. A. *J. Am. Chem. Soc.* **1986**, *108*, 2222. Wheeler, R. A.; Hoffmann, R.; Strähle, J. *J. Am. Chem. Soc.* **1986**, *108*, 5381.

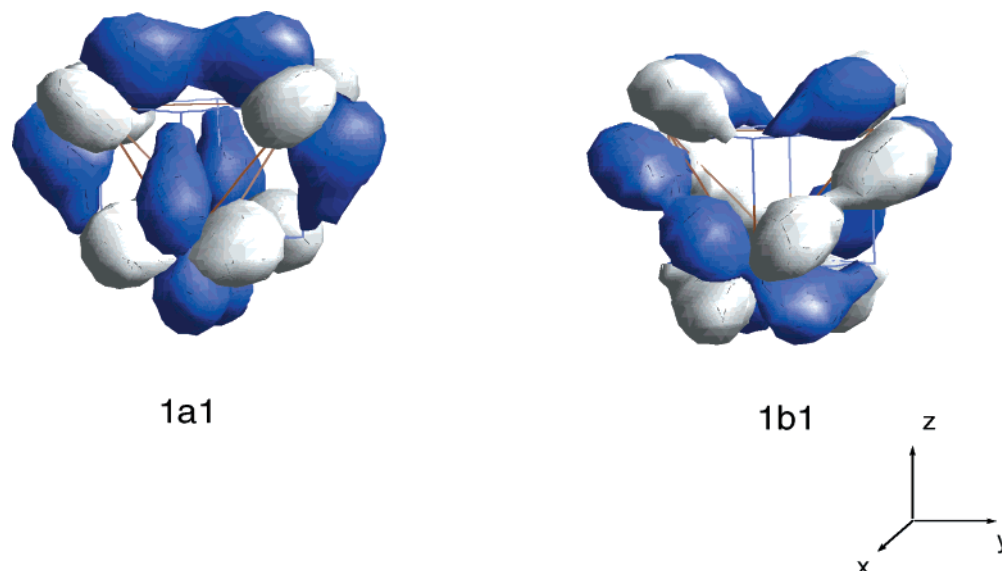


Figure 2. 3D plot of the occupied e-like metal orbitals ($1a_1 + 1b_1$ in the actual D_{2d} symmetry) in the cubane conformation of the complex $[(\eta\text{-C}_5\text{H}_5)\text{V}(\mu_3\text{-N})]_4$.

geometry. The computed bond lengths of 2.675 and 2.678 Å for V–V distances, and of 1.875 Å for V–N bonds, exactly coincide with the X-ray values of 2.674 and 1.87 Å. The computed distance between the vanadium atom and the centroid of the Cp ring is 2.038 Å, also very close to the experimental value of 2.01 Å.⁵ One of the structural points of interest in this vanadium cluster is the presence of short V–V distances. The four metal electrons are in two quasi-degenerate orbitals of symmetry a_1 and b_1 (e-like orbitals). A 3D drawing of these two molecular orbitals (Figure 2) shows a certain vanadium–vanadium overlap in some regions of the cube. Should the short metal–metal distances be assigned to this bonding character? To determine if there is a relationship between the number of metal electrons and the size of the cube, we have optimized the structure of the doubly ionized cluster $[(\eta\text{-C}_5\text{H}_5)\text{V}(\mu_3\text{-N})]_4^{2+}$. After removing two metal electrons from the cluster the V–N and V–V distances slightly increase (0.007 and 0.03 Å, respectively). A first analysis of these values could suggest that the changes in the V–V separations are quite small and could be correlated with a low overlap between the vanadium orbitals. Secondary effects due to ionization could also be responsible for small distortions of the cubic structure. The electrostatic repulsion due to the positive charges on the metal atoms will increase the V–V distances, whereas the same positive charges tend to strengthen the vanadium–nitrogen σ bonds and are then expected to contract the cube. To sum up, we believe that the small size of the cube in the $[(\eta\text{-C}_5\text{H}_5)\text{V}(\mu_3\text{-N})]_4$ cluster is mainly due to the presence of strong metal–ligand bonds, as pointed out by Bottomley and co-workers,⁵ but the possible contribution of metal–metal bonding interactions should not be neglected. More important in view of the discussion below are the geometry changes induced by the addition of one electron to the unoccupied a_1 orbital (see Figure 3). After reoptimizing the geometry, the cube becomes somewhat distorted since the V–N bond lengths slightly increase (~ 0.02 Å), whereas the V–V distances become 0.05 Å shorter than in the neutral cluster. This contraction is obtained despite the opposite trend induced by

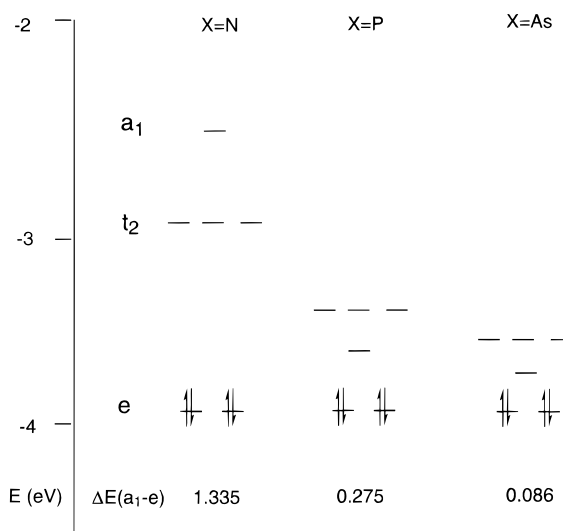
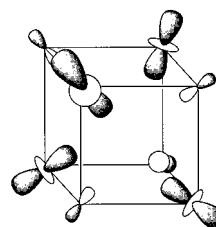


Figure 3. Energy diagram of the frontier orbitals obtained for $[(\eta\text{-C}_5\text{H}_5)\text{V}(\mu_3\text{-X})]_4$ with X = N, P, and As, assuming for all three complexes the singlet ground-state configuration computed for the vanadium nitride cluster ($e^4t_2^0a_1^0$). The symmetry labels refer to the pseudo-tetrahedral symmetry of the M_4X_4 core.

Chart 3



the combined effects of the electrostatic and the Pauli repulsion. This is an indication of the strong metal–metal bonding nature of the a_1 orbital, schematized in Chart 3. Quite logically, a still enhanced distortion can be expected from the transfer of one electron from the e-like orbitals to the a_1 level (see next section and Table 2). Note that a similar in-phase combination of four d_{z^2} -

Table 1. Relative Energies (in kcal mol⁻¹) of the Singlet and Triplet Lowest States for the Cubane Clusters [(η -C₅H₅)V(μ_3 -X)]₄ (X = N, P, and As)

occupation ^a	state	X = N	X = P	X = As
1a ₁ ² 1b ₁ ² (e ⁴)	singlet	0.0	2.8	13.8
1a ₁ ² 2a ₁ ²	singlet	47.1	0.9	1.2
1a ₁ ² 1b ₁ ¹ 2a ₁ ¹ (e ³ a ₁ ¹)	triplet	13.8	0.0	0.0

^a Distribution of the four metal electrons among the lowest metal orbitals. The electronic configurations have been classified using the actual symmetry of the molecule (*D*_{2d}). In Tables 1 and 2 labels in parentheses identify the associated configuration in the undistorted *T_d* cube.

Table 2. Selected Bond Distances^a and Bond Angles^a for [(η -C₅H₅)V(μ_3 -X)]₄ (X = P and As) Computed for the 1a₁²1b₁² (e⁴), 1a₁²1b₁¹2a₁¹ (e³a₁¹), and 1a₁²2a₁² Configurations (see the text)

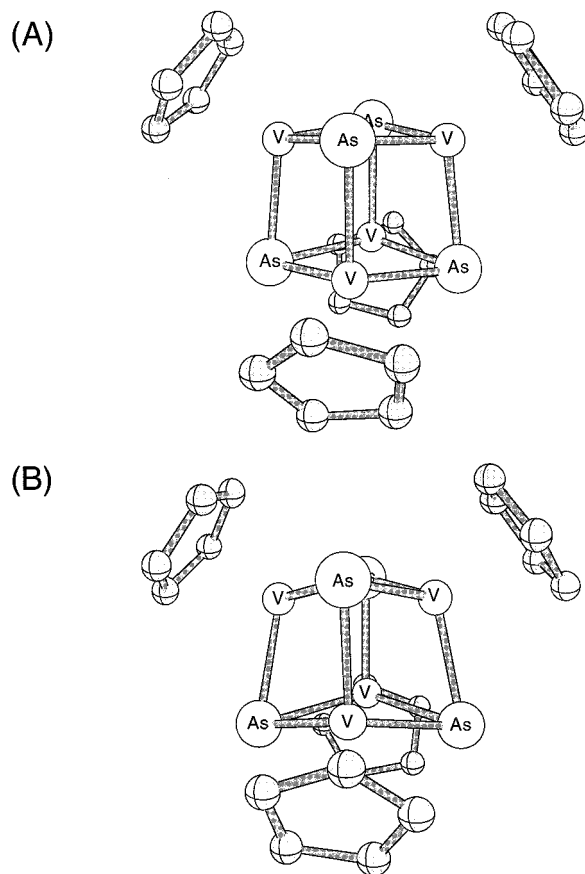
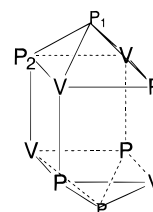
[(η -C ₅ H ₅)V(μ_3 -P)] ₄			
	1a ₁ ² 1b ₁ ²	1a ₁ ² 1b ₁ ¹ 2a ₁ ¹	1a ₁ ² 2a ₁ ²
V–P	2.31	2.33	2.34
V–V	3.07	2.97	2.80
V–P–V	83.2	79.1	72.5
P–V–P	96.3	100.1	104.5

[(η -C ₅ H ₅)V(μ_3 -As)] ₄			
	1a ₁ ² 1b ₁ ²	1a ₁ ² 1b ₁ ¹ 2a ₁ ¹	1a ₁ ² 2a ₁ ²
V–As	2.42	2.46	2.44
V–V	3.17	2.91	2.86
V–As–V	81.8	72.6	71.5
As–V–As	97.6	105.0	106.5

^a Averaged values.

like orbitals has been shown to account for the metal–metal bonding interactions in metallocarbohedrenes M₈C₁₂.³³

The Clusters [(η -C₅H₅)V(μ_3 -X)]₄, X = P, As, and [(η -C₅H₅)V(μ_3 -P)]₄(μ -P)₂. The cubane clusters [RV(μ_3 -P)]₄ and [RV(μ_3 -As)]₄ have not been synthesized yet, but the analysis of these molecules is very useful for understanding the structure and electronic properties of vanadium cubane clusters with elements of group 15. Figure 3 displays orbital energies computed for the clusters [RV(μ_3 -X)]₄ with X = N, P, and As, assuming for all three complexes the ground-state configuration e⁴t₂⁰a₁⁰ computed for the vanadium nitride cluster. Most interesting in this series of diagrams is the strong stabilization of the metal orbital with a₁ symmetry when N atoms are substituted by P or As. Hence, whereas the energy difference between the a₁ and e orbitals is 1.3 eV in [(η -C₅H₅)V(μ_3 -N)]₄, this difference drops to 0.27 eV in [(η -C₅H₅)V(μ_3 -P)]₄ and 0.09 eV in [(η -C₅H₅)V(μ_3 -As)]₄. This stabilization is assigned to the diminution of the repulsive interactions between X and the toroidal part of the pseudo-d_{z²} metal orbitals (see Chart 3) as the M–X distance increases. As a consequence of the stabilization of orbital 2a₁, the ground state for the phosphide and arsenide vanadium clusters becomes the triplet state e³a₁¹t₂⁰ (in the actual *D*_{2d} symmetry the electronic configuration is 1a₁²1b₁¹2a₁¹). For both clusters the energy of the singlet corresponding to four metal electrons in the e-like orbitals (configuration 1a₁²-1b₁² in the *D*_{2d} symmetry) is higher than that of the triplet ground state. The relative energy of this singlet with respect to the ground state was computed to be 2.8 kcal mol⁻¹ for [(η -C₅H₅)V(μ_3 -P)]₄. Despite this low energy difference, the geometries of the singlet and triplet states are relatively different. For the singlet

**Figure 4.** Optimized triplet (A) and singlet (B) structures for [(η -C₅H₅)V(μ_3 -As)]₄. The singlet state corresponds to the configuration with four electrons in the e-like metal orbitals.**Chart 4**

geometry the cube is slightly distorted and the V–P–V and P–V–P angles are ~83° and 96°, respectively. In this diamagnetic state the vanadium–vanadium distances are equal to ~3.07 Å. But if one electron from the e-like orbital is allowed to populate the a₁ orbital (or 2a₁ in the *D*_{2d} symmetry, Chart 3-like orbital) the metal–metal interactions lead to a shortening of the V–V distances by 0.1 Å (Table 2) and to a significant distortion of the cube. Similar geometrical changes were found for the [(η -C₅H₅)V(μ_3 -As)]₄ cubane cluster. In this case, the singlet–triplet energy difference was computed to be more important, 13.8 kcal mol⁻¹. As in the phosphide cluster, the geometry of the triplet state can be seen as a strongly distorted cube (see Figure 4). It is noteworthy that for both X = P and X = As the singlet state obtained by fully populating the 2a₁ orbital appears very close in energy to the triplet ground state (Table 1).

Somewhat different is the situation in the [(η -C₅H₅)V(μ_3 -P)]₄P₂ cluster, which can be described as a cube with two capping phosphorus atoms, Chart 4. Assuming that

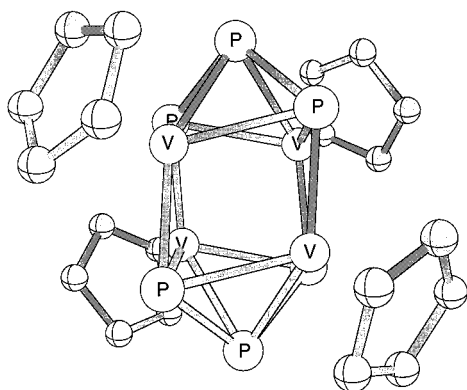


Figure 5. Structure optimized for $[(\eta\text{-C}_5\text{H}_5)\text{V}(\mu_3\text{-P})_4(\mu\text{-P})_2]$.

Table 3. Some Computed and X-ray Bond Lengths and Bond Angles for $[(\eta\text{-C}_5\text{H}_5)\text{V}(\mu_3\text{-P})_4(\mu\text{-P})_2]$

	DFT ^a	X-ray ^a
V–P ₁	2.419	2.432
V–P ₂	2.468–2.363	2.44–2.35
V–V	2.902–3.179	2.87–3.18
P ₁ –P ₂	2.242	2.179
P ₂ –P ₁ –P ₂	108.4	109.0
P ₂ –V–P ₂	94.8–105.7	92.7–106.3

^a The presence of the capping phosphorus atoms breaks the T_d symmetry of the V_4P_4 core and generates two sets of V–V and V–P₂ distances (see Scheme 4 for notation). The shortest V–V and V–P₂ distances belong to the uncapped faces.

the P–P bonds have covalent nature and that the P → V bonds are coordinative bonds, the phosphorus at the vertexes of the cube are formally P^{2–} ligands, whereas the capping phosphorus are P[–] ligands. Therefore, it appears from an elemental electron counting that this cluster has six metal electrons. In full agreement with this formal distribution, the ground state computed for $[(\eta\text{-C}_5\text{H}_5)\text{V}(\mu_3\text{-P})_4\text{P}_2]$ under the constraints of D_2 symmetry is a singlet corresponding to the $1a^22a^23a^2$ configuration for the metal electrons. The electron distribution generated by those three orbitals is very similar to the electron density associated with the $e+a_1$ orbitals in the cubane conformation of cluster $[(\eta\text{-C}_5\text{H}_5)\text{V}(\mu_3\text{-X})_4]$. Figure 5 shows the optimized molecular geometry, and Table 3 compares some computed and experimental geometrical parameters. The important distortion of the cube in $[(\eta\text{-C}_5\text{H}_5)\text{V}(\mu_3\text{-P})_4(\mu\text{-P})_2]$ results in part from the presence of two electrons in the vanadium bonding Chart 3-like orbital, which tends to reduce all metal–metal distances by attracting the vanadium atoms toward the center of the cube, as discussed for $[(\eta\text{-C}_5\text{H}_5)\text{V}(\mu_3\text{-P})_4]$ and $[(\eta\text{-C}_5\text{H}_5)\text{V}(\mu_3\text{-As})_4]$. The capping phosphorus P₁ is bonded to two P₂ and two vanadium atoms with relatively short distances. To analyze the bonding within the (P)₃ fragments as well as between these fragments and the metal framework, we have computed the Laplacian of the charge density in a plane that contains the two capping P, two V, and two P atoms of the cuboid (Figure 6). The internuclear charge density concentration linking P₁ and P₂ is typical of a covalent interaction,³⁴ whereas the presence of the P lone pairs directed toward the V atoms is a clear indication of the donor nature of the phosphorus → metal bonds.³⁵ Note the existence in both types of phosphorus atoms of a

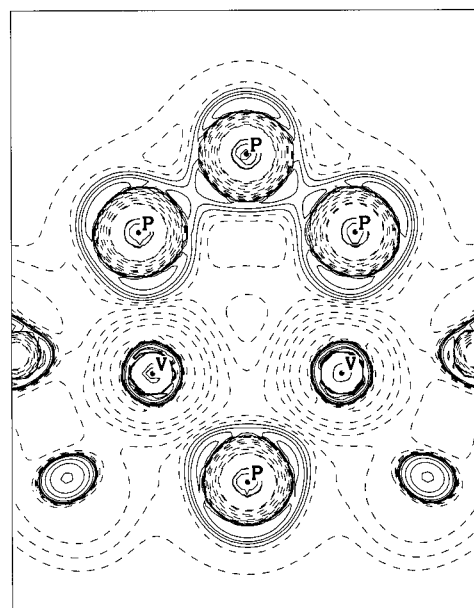


Figure 6. Laplacian of the charge density for $[(\eta\text{-C}_5\text{H}_5)\text{V}(\mu_3\text{-P})_4(\mu\text{-P})_2]$ in a plane containing the two capping phosphorus, two vanadium, and two capped phosphorus atoms. This map illustrates the covalent and coordinative nature of the P–P and P → V bonds, respectively.

fifth region of charge accumulation opposite the square pyramid of the P–V and P–P bonds.

[Cl₃MoN]₄. The structure of $[\text{Cl}_3\text{MoN}]_4$, known since 1970, appears as a ring composed of four series of Mo≡N–Mo bridges with pairs of Mo–N bond distances of 1.66 and 2.13 Å.³⁶ The metallic center, which has a distorted trigonal bipyramid coordination, can incorporate an additional ligand to the coordination sphere. The $[\text{Cl}_3\text{MoN}\cdot\text{OPCl}_3]_4$ adduct³⁷ is one of the various tetrameric cyclic structures characterized in the 1970s in which the coordination around the molybdenum is octahedral.³⁸ We have chosen to investigate the $[\text{Cl}_3\text{MoN}]_4$ complex in the second part of this work in order to compare the hypothetical cubane form with the ring structure and to delineate the factors that govern the formation of one or the other isomer.

The present DFT calculations reproduce quite well the observed distortion resulting from the breaking of the D_{4h} symmetry. The values of 1.70 and 2.18 Å computed for the Mo–N bond lengths are in keeping with the distances of 1.66 and 2.13 Å observed from X-rays and assigned to a triple and to a single Mo–N bond, respectively. Molecular orbitals for closely related systems were analyzed in detail by Wheeler and co-workers by means of extended Hückel calculations.³⁹ More recently, Schoeller and Sundermann⁴⁰ reported ab initio and DFT calculations on the Cl_3MoN tetramers (M = Cr, Mo, W) in the square planar conformation of the M_4N_4 framework. This study showed that the bonding energy of $[\text{Cl}_3\text{MoN}]_4$ with respect to the four isolated monomers is relatively weak ($\sim 29 \text{ kcal mol}^{-1}$ from DFT/B3LYP/ECP calculations carried out with valence basis sets including polarization functions on nonmetal atoms).⁴⁰ It was concluded that the bonding in the cyclic $[\text{Cl}_3\text{MN}]_n$ polymers results from weak donor–acceptor interactions between the nitrogen lone pair of a monomer and an empty d orbital centered on the metal of the next fragment.

(40) Schoeller, W. W.; Sundermann, A. *Inorg. Chem.* **1998**, *37*, 3034.

Table 4. Decomposition of the Binding Energy (BE) Calculated for the Cubane (D_{2d}) and for the Square Planar (C_{4v}) Forms of $[\text{TiNCp}]_4$ and $[\text{MoCl}_3\text{N}]_4$ with Respect to Four Isolated, Fully Relaxed Monomers (all values in eV)

	$[\text{TiNCp}]_4$		$[\text{MoCl}_3\text{N}]_4$	
	D_{2d}	C_{4v}	D_{2d}	C_{4v}
FE ^a	-73.05	-73.81	-21.74	-25.44
FIE ^b	-23.22	-14.89	-13.85	-3.90
steric repulsion	+10.3	+6.52	+25.4	+5.84
electron reorganization	-33.5	-21.41	-39.2	-9.74
FDE ^c	+5.83	+2.81	+17.30	+2.50
BE ^d	-17.38	-12.07	+3.45	-1.40

^a The fragment energy is the energy of an isolated monomer calculated assuming its structure optimized in the cluster. Energies in DFT methods are usually given as binding energies with respect to the sum of energies of the isolated atoms. Energies of the relaxed fragments FE_{relax} for TiNCp and MoCl_3N are -74.51 and -26.06 eV, respectively. ^b The fragment interaction energy (FIE) is the energy assigned to the interaction between the four mononuclear units. It is globally attractive and can be decomposed into the sum of an attractive term referred to as the electron reorganization term (but also accounting for the Coulombic attraction) and of a repulsive term accounting for the steric and Pauli interactions. ^c The fragment deformation energy (FDE) represents the energy requested to transform the four fragments from their equilibrium structure to the geometry of the fragment in the complex. It is given by $\text{FDE} = 4(\text{FE} - \text{FE}_{\text{relax}})$. ^d The total binding energy term (BE) corresponds to the difference between the total energy of the complex and four times that of a relaxed fragment. It is also given by the sum of $\text{FIE} + \text{FDE}$.

At variance with $[\text{TiNCp}]_4$, the isoelectronic molybdenum tetramer $[\text{Cl}_3\text{MoN}]_4$ is much more stable in the square planar (or C_{4v}) than in the cubane-like (or D_{2d}) conformation. The energy difference is very high, 112 kcal mol⁻¹. Let us remember that the preference of $[\text{TiNCp}]_4$ for the opposite conformation was also based upon a great energy difference (123 kcal mol⁻¹). Surprisingly, the reasons for these markedly opposite preferences are not easily outlined. To get a better understanding of the electronic and steric strain associated with each conformation state, we have calculated the *fragment energies* (FE) of the isolated TiNCp and MoNCl_3 monomers in the geometry they adopt in the ring-like and in the cubane-like tetramers. The *fragment deformation energy* (FDE) is defined as 4 times the energy difference between the fragment energy and the energy of the corresponding monomer in its optimal, fully relaxed conformation. The FDE therefore represents the energy required for transforming four noninteracting fragments from their equilibrium structure to the geometry best suited to each conformation of the tetramer (Table 4). The other contribution to the binding energy of the complex is the *fragment interaction energy* (FIE) accounting for the interactions among the four monomers. The FIE itself can be decomposed into (i) a repulsive term, accounting for both the steric strain and the Pauli repulsion and (ii) an attractive contribution which gathers the Coulombic interactions (mutual polarization and orbital interactions). These contributions and the resulting binding energy, defined as

$$\text{BE} = \text{FDE} + \text{FIE}$$

are displayed in Table 4.

An analysis restricted to the FIE components shows that the D_{2d} structure implies for both complexes a large electronic reorganization. The benefit of this redistribu-

tion of the electron density is however partly offset in the molybdenum cubane-like tetramer by a high value of the steric and Pauli repulsion (Table 4). The repulsive term remains moderate in the cubic form of $[\text{TiNCp}]_4$, which displays the largest attractive fragment interaction energy (-23.2 eV, Table 4). If we now consider the isomers with a square planar framework, Table 4 shows that the attractive term is also relatively high for the titanium complex, in relation to the strong *interfragment* Ti-N bonds. Since the steric + Pauli repulsion is lower in the C_{4v} framework than in the cube, as can be expected for this less compact conformation, the FIE ranks second largest (-14.9 eV). The energetic balance of the fragment interactions is not so favorable in either conformation of the molybdenum tetramer. In the observed "planar" form, the attractive and the repulsive interactions are moderate, as they should be in the "weak donor-acceptor complexes" previously described by Schoeller and Sundermann.⁴⁰ The interaction balance eventually remains attractive, but the FIE does not exceed -3.9 eV. The balance is more favorable in the cubic-like conformation (-13.8 eV) despite an extremely large repulsive term (Table 4).

At variance with the case of the titanium tetramer, the FIE term alone is not sufficient to explain the high stability of the observed conformer of $[\text{Cl}_3\text{MoN}]_4$. As a matter of fact, the fragment deformation energy (FDE) is the key factor inducing the relative stability of the molybdenum complex in its square planar conformation. In the form with C_{4v} symmetry, the formation of the tetramer does not require significant changes either in the $\text{Mo}\equiv\text{N}$ bond length or in the Cl-Mo-N angles. Thus, the fragment deformation energy associated with the ring formation is quite small (+2.50 eV), and the total binding energy remains slightly stabilizing. The overall binding energy (-1.40 eV = -32.3 kcal mol⁻¹) is comparable to the value obtained by Schoeller and Sundermann with their best basis set (-28.6 kcal mol⁻¹).⁴⁰ In contrast to the case of the planar form, the FDE is especially high in the cubane structure (+17.3 eV). This is sufficient to offset the FIE and to yield a repulsive binding energy (+3.45 eV) with respect to the isolated monomers. What is the origin of this huge FDE term? It should be assigned to the combination of two structural characters, both highly penalizing, encountered in the conformation adopted by the NMoCl_3 fragment in the D_{2d} complex. First comes the stretching of the Mo-N bond from 1.665 to 2.05 Å. The Mo-N stretching in the four fragments contributes ~5 eV to the FDE. The second transformation relates to the orientation of the MoCl_3 tripod with respect to the Mo-N bond. The relaxed NMoCl_3 monomer has a perfect C_{3v} symmetry, with all N-Mo-Cl angles equal to 104.8°. Those angles are only slightly modified in the ring-like tetramer (102.8° and 104.9°). In the cubane-like tetramer, the octahedral coordination of the metal requires a dramatic rotation of the Cl_3 tripod around an axis that contains the metal atom and is perpendicular to one N-Mo-Cl plane (Chart 5). The angular amplitude of the rotation is ~70° and the resulting N-Mo-Cl angles in the D_{2d} complex are 176°, 94°, and 93°. The energy cost of this tilting is 2.32 eV *per monomer* and therefore accounts for the rest of the FDE. It is finally important to note that, at variance with

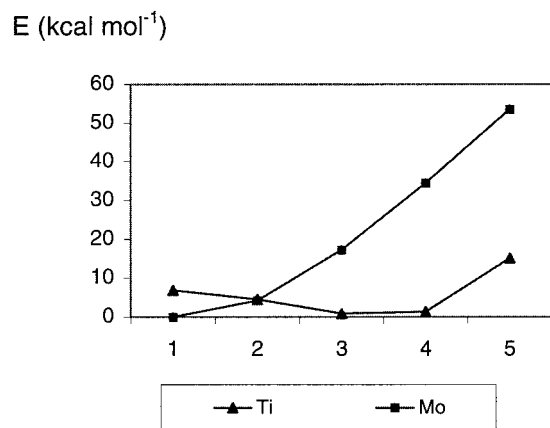
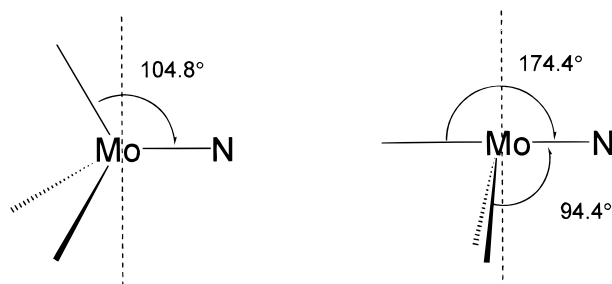


Figure 7. Potential energy curves associated (i) with the bending of the N–Ti–Ω angle in NTiCp (Ω is the centroid of the Cp ring) and (ii) with the rotation of the Cl₃ tripod around an axis containing Mo and perpendicular to one N–Mo–Cl plane in NMoCl₃ (see Scheme 5).

Chart 5



NMoCl₃, the relaxed CpTiN monomer is not linear, but bent with a N–Ti–Ω angle close to 130° (Ω is the centroid of the Cp ring). The transition to an octahedral coordination in the cubane-like tetramer does not require a substantial modification of this tilt angle. The stretching of the Ti–N bond therefore remains the only deformation inducing a large energy cost, and the FDE in the *D*_{2d} form of [TiNCp]₄ is limited to 5.8 eV (Table 4).

It is finally interesting to compare the response of the NM(L) monomers (M, L = Ti, Cp; Mo, Cl₃) to the tilting of the M–L fragments described above (Figure 7). The potential energy curve obtained for the rotation of the Cl₃ tripod is extremely steep, as expected from the analysis of the FDE term (Table 4). This means that the Cl₃Mo≡N molecule is markedly rigid, and this can be interpreted as the sign of a certain stability of the monomeric species. This is confirmed by the calculations of Schoeller and Sundermann⁴⁰ and by those of the present work, showing that the thermodynamic balance of polymerization is unfavorable for a cubane-like form and no more than weakly exothermic for polymers with ring-like (MoN)_n frameworks (*n* = 3–6). The experimental characterization of Cl₃Mo≡N⁴¹ despite the strongly unsaturated electronic environment of the metal and the synthesis of Cl₄Mo≡N⁴² and that of other mononuclear nitrido complexes containing a metal

atom of group 6^{38,43,44} give support to this interpretation. The behavior of NTiCp is opposite: the titanium monomer appears fluxional since the N–Ti–Ω angle can be varied between 110° and 180° at a cost limited to 7 kcal mol^{–1} (Figure 7). As for Cl₃Mo≡N but in the opposite way, the flexibility of NTiCp can be correlated with its instability as a monomer: the energetic balance of Table 4 shows that NTiCp has a strong tendency to polymerize. On the experimental side, it seems that no monometallic nitrido complex has been reported to date with metals of group 4, and only two such complexes have been characterized with elements of group 5.⁴⁵

Summary and Conclusion

The DFT calculations carried out on the cubane and on the ring-like structures of [CpTiN]₄ and [Cl₃MoN]₄ illustrate the strikingly different behavior of these two isoelectronic clusters. Whereas the cubane form of [CpTiN]₄ outperforms the square planar isomer by 123 kcal mol^{–1}, the energy balance between the two structures is practically opposite for the isoelectronic cluster [Cl₃MoN]₄. Other differences have been outlined. In [Cl₃MoN]₄ the four fragments get assembled into the square planar structure by means of weak donor–acceptor interactions with little geometric reorganization and moderate amounts of energy involved in the interfragment interactions, either attractive (Coulombic interaction, electron reorganization) or repulsive (steric strain, Pauli repulsion). The formation of the cubane isomer, which would require an important structural rearrangement of the fragments, is energetically unfavorable, even with respect to the isolated monomers. This has to do with the rigidity of the Cl₃MoN monomer, which is highly penalized by the reorganization of the coordination sphere. In contrast to that, the bent and flexible structure of the CpTiN monomer can adapt at low cost and easily takes place into a cubane framework, resulting in a high binding energy for the tetramer. An extension of that study to the vanadium clusters with cubane-like framework, (CpVX)₄ (X = N, P, and As), and to the dicapped derivative of the vanadium–phosphorus cluster (CpVP)₄P₂ has enlightened the importance of the metal–metal interactions in some of those compounds and their influence on the geometry of the V₄X₄ cubic-like framework. Let us finally mention the very recent

(43) Schweda, E.; Strähle, J. *Z. Naturforsch.* **1980**, *35b*, 1146. Chisholm, M. H.; Hoffman, D. M.; Huffman, J. C. *Inorg. Chem.* **1983**, *22*, 2903. Mindiola, D. J.; Cummins, C. C. *Angew. Chem., Int. Ed. Engl.* **1998**, *37*, 945. Fenske, D.; Frankenau, A.; Dehnicke, K. *Z. Anorg. Allg. Chem.* **1989**, *574*, 14. Caulton, K. G.; Chisholm, M. H.; Doherty, S.; Folting, K. *Organometallics* **1995**, *14*, 2585. Chiu, H.-T.; Chen, Y.-P.; Chuang, S.-H.; Jen, J.-S.; Lee, G.-H.; Peng, S.-M. *J. Chem. Soc., Chem. Commun.* **1996**, 139.

(44) Rentschler, E.; Dehnicke, K. *Z. Naturforsch.* **1993**, *48b*, 1841. Young, C. G.; Janos, F.; Bruck, M. A.; Wexler, P. A.; Enemark, J. H. *Aust. J. Chem.* **1990**, *43*, 1347. Azuma, N.; Imori, Y.; Yoshida, H.; Tajima, K.; Li, Y.; Yamauchi, J. *Inorg. Chim. Acta* **1997**, *266*, 29. Laplaza, C. E.; Johnson, M. J. A.; Peters, J. C.; Odom, A. L.; Kim, E.; Cummins, C. C.; George, G. N.; Pickering, I. J. *J. Am. Chem. Soc.* **1996**, *118*, 8623. Odom, A. L.; Cummins, C. C.; Protasiewicz, J. D. *J. Am. Chem. Soc.* **1995**, *117*, 6613. Kim, J. C.; Rees, W. S., Jr.; Goedken, V. L. *Inorg. Chem.* **1994**, *33*, 3191.

(45) Willing, W.; Christophersen, R.; Müller, U.; Dehnicke, K. *Z. Anorg. Allg. Chem.* **1987**, *555*, 16. Critchlow, S. C.; Lerchen, M. E.; Smith, R. C.; Doherty, N. M. *J. Am. Chem. Soc.* **1988**, *110*, 8071.

(46) McGrady, J. E. *J. Chem. Soc., Dalton Trans.* **1999**, 1393.

(47) Abarca, A.; Galakhov, M.; Gómez-Sal P.; Martín A.; Mena, M.; Poblet, J.-M.; Santamaría, C.; Sarasa, J. P. *Angew. Chem., Int. Ed. Engl.* **2000**, *39*, 534.

(41) Dehnicke, K.; Strähle, J. *Z. Anorg. Allg. Chem.* **1965**, *339*, 171.

(42) Müller, U.; Schweda, E.; Strähle, J. *Z. Naturforsch.* **1983**, *38b*, 1299. Jones, P. G.; Schroeder, T.; Sheldrick, G. M. *Acta Crystallogr.* **1987**, *43C*, 355. Knopp, B.; Lörcher, K.-P.; Strähle, J. *Z. Naturforsch.* **1977**, *32b*, 1361.

work by McGrady, who emphasized the importance of the metal–metal bonds in closely related complexes with cubane-like structure, $(\text{CpMoX})_4$ ($\text{X} = \text{O}$ and S).⁴⁶ The delocalization of the charge density of the metal carbonyl fragment in the heterometallic cubanes $[\{\text{Ti}_3\text{-Cp}^*_3(\mu_3\text{-CR})\}(\mu_3\text{-O})_3\{\text{Mo}(\text{CO})_3\}]$ ($\text{R} = \text{H}$, Me) and $[\{\text{Ti}_3\text{-Cp}^*_3(\mu_3\text{-N})\}(\mu_3\text{-NH})_3\{\text{M}(\text{CO})_3\}]$ ($\text{M} = \text{Cr}$, Mo , W) has also been described in terms of metal–metal couplings.⁴⁷

Acknowledgment. All calculations have been carried out on workstations purchased with funds provided by the DGICYT of the Government of Spain and by the CIRIT of Generalitat of Catalunya (Grants No. PB98-0916-C02-02 and SGR99-0182). We also thank the Universidad de Zaragoza for Grant No. 232-65.

OM990986P